

Radiation heat-transfer model for the ablation zone of low-density carbon-resin composites

A.J. van Eekelen*

SAMTECH, Liège, B-4031, Belgium

J. Lachaud†

NASA Ames Research Center, Moffett Field, CA, 94035, USA

Direct numerical simulations of radiation heat-transfer have enabled the validation of a semi-analytical model for the effective radiative conductivity of two-dimensional carbon-fiber preforms. The effective conductivity is shown to be a function of three parameters: the local temperature, the extinction coefficient, and the sample thickness. The integration of the proposed model in state-of-the-art ablation tools is relatively simple because only the effective conductivity needs to be modified (the formulation of the energy equation is not modified). This fundamental study has been applied to ablation. In the ablation zone of low-density carbon-resin composites, the matrix is removed and the carbon fibers lie unprotected. The effective radiative conductivity is found to be about twice as large when the matrix is removed. Although the ablation zone is very thin, its presence is shown to slightly modify the internal temperature profile.

Nomenclature

A_i	=	surface, m^2	ϵ_σ	=	emissivity, -
c	=	capacity, $\text{J}/(\text{kg}\cdot\text{K})$	ρ	=	density, $\text{kg}/(\text{m}^3)$
d	=	distance, m	λ	=	conductivity, $\text{W}/(\text{m}\cdot\text{K})$
F_{ij}	=	view-factor, -	σ	=	Stefan-Boltzmann constant, $5.67 \cdot 10^{-8} \text{ W}/(\text{m}^2 \cdot \text{K}^4)$
H_i	=	incident flux, $\text{W}/(\text{m}^2)$	σ_{ext}	=	specific extinction coefficient, m^2/kg
k	=	correlation coefficient, -	<i>Sub/Super-script</i>		
\bar{k}	=	average correlation coefficient, -	0	=	apparent value
q	=	heat flux, $\text{W}/(\text{m}^2)$	1,2	=	walls
R_i	=	radiosity, $\text{W}/(\text{m}^2)$	i	=	fiber faces
T	=	temperature, K	r	=	radiative
Δx	=	length of the model, m	λ	=	conductive
Δy	=	height of the model, m			
Δz	=	depth of the model, m			

I. Introduction

A CRITICAL problem in the design of Thermal Protection Systems (TPS) for planetary entry-vehicles is the choice of a heat shield material and its associated material response model. For sample-return missions, low-density carbon-resin (C/R) composites have been introduced and validated in flight by the Stardust mission.¹ The use of this new class of ablative materials is being seriously considered for numerous

*Product manager, Analysis department, Rue des Chasseurs-Ardennais 8, and AIAA member.

†NASA Postdoctoral Program Fellow at NASA Ames Research Center, Aerothermodynamics Branch, Mail Stop 230-3.

Copyright © 2010 by the American Institute of Aeronautics and Astronautics, Inc. The U.S. Government has a royalty-free license to exercise all rights under the copyright claimed herein for Governmental purposes. All other rights are reserved by the copyright owner.

forthcoming missions. PICA, the low density C/R developed at NASA Ames and used for Stardust, has been selected for the Mars Science Laboratory (MSL) heat shield. PICA-X has been developed by SpaceX (Space Exploration Technologies Corp.) with the assistance of NASA to protect the Dragon capsule during re-entry^a. The European Space Agency (ESA) is currently supporting the development of a light weight C/R ablator that could be used for sample return missions.² The density of these materials lies around $300 \text{ kg}\cdot\text{m}^{-3}$. The carbon preform volume fraction is about 0.1. The density of carbon fibers typically ranges between 1600 and $2000 \text{ kg}\cdot\text{m}^{-3}$, depending on the fabrication process and the nature of the precursor. The carbon fiber preform accounts for about 60% in the overall material density, but occupies only 10% of the volume. The carbon fiber preform is a very porous material that does not have excellent ablative properties. Therefore, the preform is impregnated in phenolic-formaldehyde resin in order to: (1) improve the mechanical properties of the virgin material, (2) benefit from the globally endothermic pyrolysis of the resin, (3) produce pyrolysis gases (blockage of the heat flux at the solid/fluid interface), (4) limit radiation heat-transfer (significant above 800 K).

During Stardust post-flight analyses,¹ an unexpected drop in density was measured under the surface in a zone of 0.5 mm, strongly suggesting that ablation may have occurred in volume in the char layer.^{3,4} Scanning electron micrographs show that the subsurface carbonized resin has been removed leaving the fiber preform unprotected.¹ The objective of this study is to develop a radiation heat-transfer model for thin layers of low-density carbon-fiber preforms (in order to maintain the accuracy of material response models when the protective matrix has been removed) and to test this model.

Radiation through fibrous materials has been the subject of numerous investigations.^{6,7} Among other applications, we find LI-900,^{5,6,9,10} one of the space shuttle's tile materials. Models with different degree of complexity and accuracy have been proposed. They range from semi-analytical models anchored by experimental data⁸ to an accurate modeling of the radiative energy transport through an absorbing and scattering medium.⁷ The later method is based on the exact formulation of the scattering by a single fiber. The effective properties of a medium made of randomly distributed fibers is then estimated analytically by volume averaging. This method gives excellent results but is limited to materials with an homogeneous distribution of straight fibers. We would like to take advantage of three-dimensional micro-tomographies images to estimate and understand better the properties of the fiber preform. We shall start using direct numerical simulation at microscopic (fiber) scale to analyze, understand and model the radiative behavior of carbon-fiber preforms. As a first step, we will use a 2D model. The fiber preform will be modeled as a random array of non-overlapping cylinders parallel to the surface.

The article is organized as follows. In the second section, the model and the simulation tool are presented. A semi-analytical model for the effective conductivity due to radiative transfer is proposed. The idea is to produce a simple phenomenological model that can be integrated in state-of-the-art material-response codes. In the third section, the parameters of the phenomenological model are obtained from direct numerical simulations in steady state. In the fourth section, the phenomenological model is compared to direct numerical simulations in the transient regime. In the fifth section, the integration of the phenomenological model in material response codes is discussed and a preliminary simulation is presented.

II. Model and simulation tool

A. Material model

In order to minimize the effective conductivity of the preform, a fiber orientation parallel to the surface of the thermal protection system (TPS) is preferred in actual materials. As a first step, we shall also consider that the fibers are parallel to each other in order to reduce the actual 3D problem to a 2D problem. We will use the following fiber properties: conductivity, $\lambda = 10 \text{ W}/(\text{m}\cdot\text{K})$; specific heat capacity, $c = 1000 \text{ J}/(\text{kg}\cdot\text{K})$; density, $\rho = 1800 \text{ kg}/\text{m}^3$; and emissivity, $\epsilon_\sigma = 0.85$ (gray body). The fibers are treated as perfect cylinders with a diameter of $10 \mu\text{m}$. In the 2D material model, the fiber volume fraction is 0.1. Non-overlapping fibers are randomly placed in a 2D box using a Monte-Carlo procedure until the required volume fraction is obtained (Fig. 1).

^a<http://www.spacex.com/press.php?page=20090223>



Figure 1. Random distribution of fibers between two walls ($\Delta x = 1mm$).

B. Physical model and associated simulation tool

An electromagnetic wave or photon passing through the immediate vicinity of a fiber is either absorbed or scattered. The scattering is due to three separate phenomena, namely, (i) diffraction (waves never come into contact with the fiber, but their direction of propagation is altered by the presence of the fiber), (ii) reflection (wave reflected from the surface of the fiber), and (iii) refraction (wave that penetrate into the fiber and, after partial absorption, reemerge traveling into a different direction).¹² Because carbon fibers are opaque, there is no refraction. The surface of the fibers will be rough, so we can assume that the reflection is diffuse. Diffraction can only be neglected when the wave length is small compared to the fiber diameter. In the case of fibrous media, the size parameter x is defined as:

$$x = \frac{d \cdot \pi}{\lambda} \quad (1)$$

where the fiber diameter d equals $10 \mu m$ and where λ is the wavelength of interest. In general, diffraction is negligible for $x \geq 10$. But the work of Lee⁵ has shown that diffraction, for randomly oriented fibers, has a negligible effect on effective heat transfer for values of x larger than unity. As a consequence, we may then neglect diffraction for wavelengths smaller than $\lambda_{lim} = 31.4 \mu m$. According to Plank's law, 99% of the energy of a black (or gray) body is emitted at wavelength smaller than $\lambda_{lim} = 31.4 \mu m$ for temperatures higher than about $700 K$. Radiative heat transfer is small compared to conduction heat transfer for temperatures below $800 K$ in carbon preforms. Therefore, we will neglect diffraction and use a gray body diffuse radiation model. More complicated models could be used (*e.g.* specular or non-monochromatic radiation) but our first goal is to develop and test a method, and not to investigate in detail the intrinsic properties of carbon fibers.

The perimeter of each fiber is discretized in facets (or faces). View-factors, which model the energy exchange between the faces, need to be calculated between the fiber faces:

$$F_{ij} = \frac{\text{Energy absorbed by face } A_j, \text{ by direct travel}}{\text{Diffuse energy emitted by face } A_i} = \frac{1}{A_i} \int_{A_j} \int_{A_i} \frac{\cos(\theta_i) \cos(\theta_j)}{d^2} dA_i dA_j \quad (2)$$

which can be expressed both as an energy balance, or as a geometric quantity (isothermal facets). The view-factors are obtained using a collision based Monte-Carlo method, to which reciprocity and least-squares closure is applied as described by Zeeb.¹¹

In the case of diffuse gray body radiation, we can introduce the radiosity of a face R_i , that is defined as the emitted energy of the face plus the portion of the incoming radiation H_i that is reflected by the face.

$$R_i = \epsilon_\sigma \sigma T_i^4 + (1 - \epsilon_\sigma) H_i \quad (3)$$

If we write the energy balance equation for face i , as either the difference of the incident flux (H_i) and the total radiated flux (R_i), or the absorbed flux and the emitted flux, we obtain the following:

$$q_i = H_i - R_i = \epsilon_\sigma H_i - \epsilon_\sigma \sigma T_i^4 \quad (4)$$

The incident flux on face i can be expressed by the sum of all the radiosities (R_j), times the view-factors between facet i and the rest of the closed cavity.

$$H_i = \sum_{j=1}^N R_j F_{ji} \quad (5)$$

Using reciprocity ($A_i F_{ij} = A_j F_{ji}$) and closure ($\sum_{j=1}^N F_{ij} = 1$) the final balance equation for facet i equals:

$$\sum_{j=1}^N F_{ij} (R_j - R_i) + \frac{\epsilon_\sigma}{1 - \epsilon_\sigma} (\sigma T_i^4 - R_i) = 0 \quad (6)$$

This formulation is known as the electrical analogy formulation for radiation heat exchange. It is described in detail by Modest.¹² The heat radiation equations are combined with the standard transient heat transfer equations for solids. This allows us to model the conduction and radiation problem in both transient and steady state. All the equations are implemented in the finite-element code SAMCEF, which is used for industrial applications in the aerospace industry.¹³

C. Simplified reference model

As a reference model we will take the diffuse gray radiation between two infinite parallel planes. This model is developed in order to obtain an expression between the radiation flux and the equivalent radiative conductivity λ_r . The radiation flux q_r between two infinite planes can be expressed as follows:

$$q_r = \frac{\epsilon_\sigma F_{12}}{2 - \epsilon_\sigma} \sigma [T_2^4 - T_1^4] \quad (7)$$

where T_i is the temperature of the two planes, and ϵ_σ is the emissivity. Because the planes extend to infinity, the view-factor F_{12} equals 1. If we now impose the temperatures of both planes, where $T_1 = T - \frac{1}{2}\Delta T$, and $T_2 = T + \frac{1}{2}\Delta T$, and assume that ΔT is small, the flux can be expressed as:

$$q_r = \frac{\epsilon_\sigma}{2 - \epsilon_\sigma} \sigma [4T^3 \Delta T + T(\Delta T)^3] \approx \frac{4\epsilon_\sigma}{2 - \epsilon_\sigma} \sigma T^3 \Delta T \quad (8)$$

According to Fourier's law, the conductive heat transfer in a material in steady state writes:

$$q_\lambda = -\lambda \frac{\partial T}{\partial x} = -\lambda \frac{\Delta T}{\Delta x} \quad (9)$$

where λ is the conductivity. From these two expressions, we can obtain an expression for the effective radiative conductivity, as a function of the temperature T and the model length Δx .

$$\lambda_r = \frac{4\epsilon_\sigma}{2 - \epsilon_\sigma} \sigma T^3 \Delta x \quad (10)$$

In this paper we will calculate the effective conductivity in the presence of fibers. In order to do this we will modify the above expression and introduce an unknown parameter k .

$$\lambda_r = \frac{k\epsilon_\sigma}{2 - \epsilon_\sigma} \sigma T^3 \Delta x \quad (11)$$

Where k will be a parameter that depends on the distance and the geometry of the fibers between the two plates, which will be limited by an upper bound ($k = 4$).

D. Equivalent conductivity model

Let us make the hypothesis of Deissler;¹⁴ that is, we shall assume that there are 2 imaginary walls on the right hand side and on the left hand side of the box containing the fibers (Fig. 1). Both the fibers and the walls will have the same emissivity ϵ_σ . The model in Fig. 1 has four symmetry planes (fully specular surfaces), that will extend the model from $-\infty$ to $+\infty$ in both the y - and z -direction. Under the hypothesis of Rosseland (optically thick medium), it is possible to show that the effective conductivity may be expressed as a function of the emissivity (ϵ_σ) and the thickness of the model (Δx):⁸

$$\lambda_r = \frac{4\epsilon_\sigma \sigma T^3 \Delta x}{(2 - \epsilon_\sigma) + \sigma_{ext} \epsilon_\sigma \rho_0 \Delta x} \quad (12)$$

where ρ_0 is the apparent density of the material and σ_{ext} is the specific effective extinction coefficient that must be obtained for a given fiber configuration. If we now use Eq. (11) and (12) we obtain the relation between k and Δx :

$$k = \frac{4(2 - \epsilon_\sigma)}{(2 - \epsilon_\sigma) + \sigma_{ext}\epsilon_\sigma\rho_0\Delta x} \quad (13)$$

which is the correlation formula, using the hypothesis of Rosseland and Deissler, that we will use. To complete the equations, we will write the expressing for the equivalent radiation heat flux q_r :

$$q_r = -\frac{k\epsilon_\sigma}{2 - \epsilon_\sigma}\sigma T^3\Delta x\frac{\Delta T}{\Delta x} = -\frac{k\epsilon_\sigma}{2 - \epsilon_\sigma}\sigma T^3\Delta T \quad (14)$$

III. Steady-state and transient analyses

TWO types of analyses are performed in this section. The first analysis aims at determining the effective radiative conductivity of the fiber preform from a steady state calculation. The objective of the second analysis is to study the validity of the effective conductivity model in transient regime.

A. Steady state analysis

For the steady state analysis we will impose the temperature on both sides of the model. This will result in a known temperature difference ΔT over the model for a given temperature T ($= (T_1 + T_2)/2$). This analysis will be repeated for different temperatures T between 0 K and 4000 K.

1. Test-matrix

The steady state analysis is performed for 5 different configurations. All configurations have the same basic geometric layout (see Fig. 1), with a height Δy and a depth Δz of 100 μm , but with different lengths. The model in Fig. 1 is a finite element model where every fiber is modeled using approximately 55 elements.

- Configuration 1: 63 fibers with a length of $\Delta x = 0.5\text{mm}$.
- Configuration 2: 126 fibers with a length of $\Delta x = 1\text{mm}$.
- Configuration 3: 252 fibers with a length of $\Delta x = 2\text{mm}$.
- Configuration 4: 504 fibers with a length of $\Delta x = 4\text{mm}$.
- Configuration 5: 1008 fibers with a length of $\Delta x = 8\text{mm}$.

All five configurations are generated in such a way that they have the same fiber volume fraction ($\approx 9.76\%$), resulting in an apparent density ρ_0 of 175.68 kg/m^3 . For all configurations a total of 5 random geometries (seeds) are generated in order to assess the influence of the random fiber placement on the convergence of the solution.

2. Effective radiative conductivity

The average effective conductivity curves for the five configurations are plotted in Fig. 2. As expected from the form of Eq. 12, the effective conductivity features an asymptotic behavior as a function of Δx . For all five configurations the values of k are presented in Table 1. The random nature of the geometry has very little effect of the value of k . In Fig. 3, the average \bar{k} values are plotted as a function of the model length Δx . The data are perfectly fitted using Eq. (13) with an extinction coefficient σ_{ext} of 63.11 m^2/kg .

B. Transient analysis

Two models are now compared in a transient regime. The first one is the microscopic radiation model (direct numerical simulations at fiber scale). The second model is the classical macroscopic conduction model (conservation of the enthalpy and Fourier's law for conduction). The goal is to test the validity in the transient regime using the approach developed in the previous section. As indicated in the paper of

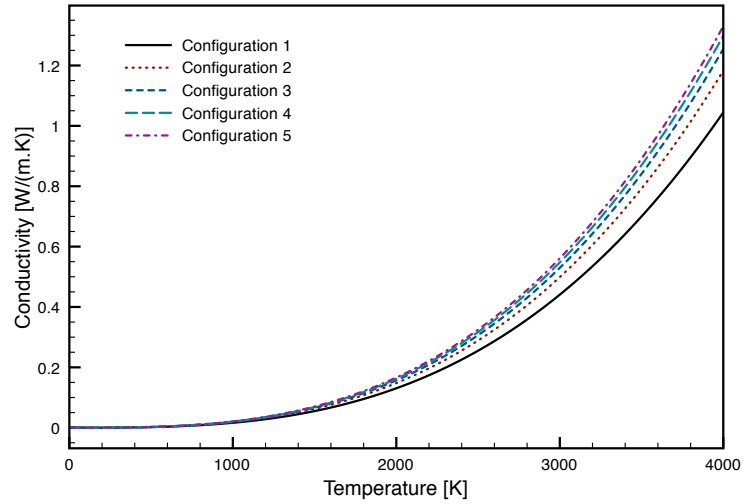


Figure 2. Average effective conductivity λ_r as a function of Temperature.

Table 1. Values of k for five random seeds.

Configuration:	1	2	3	4	5
Seed	$k[-]$				
1	0.798	0.432	0.233	0.121	0.062
2	0.785	0.445	0.233	0.121	0.062
3	0.761	0.447	0.238	0.122	0.061
4	0.796	0.447	0.232	0.122	0.062
5	0.758	0.435	0.236	0.121	0.062
$\bar{k} =$	0.779	0.441	0.234	0.121	0.062

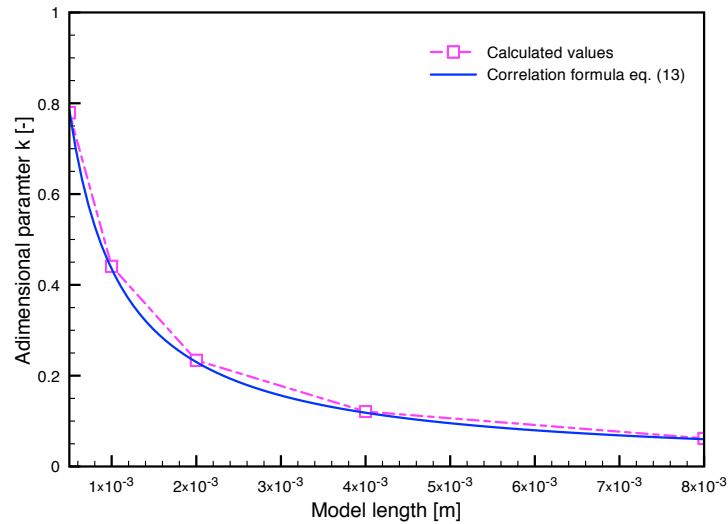


Figure 3. \bar{k} -factor as a function of Δx .

Marschall et. al.¹⁰ temperature dependent effective conductivities are not expected to correctly model the thermal transient response of a porous material, especially in high heating rate environments.

For the transient analysis we will reproduce the arc-jet heating environment test from Ref. [10]. The model is initially at 300 K. The boundary condition is a time-dependent fixed temperature (Dirichlet) on one side of the sample and an adiabatic condition (Neumann) on the other side (see Fig. 4).

1. Test-matrix

We will perform calculations for two different values of Δx . For the equivalent conductive model we will use the material properties given in Table 2. For the transient radiative model we will again perform five runs in order to obtain average transient curves. For both the radiation and the equivalent model the temperature

Table 2. Equivalent conductivity properties

calculation	Δx [m]	ϵ_σ [-]	k [-]	λ_r [W/(m.K)]
1	$4 \cdot 10^{-3}$	0.85	$1.184 \cdot 10^{-1}$	$1.985 \cdot 10^{-11} \times T^3$
2	$8 \cdot 10^{-3}$	0.85	$6.000 \cdot 10^{-2}$	$2.012 \cdot 10^{-11} \times T^3$

curves of five imaginary thermocouples were generated. The five imaginary thermocouples were positioned at the following places:

- Thermocouple 1: positioned on the left hand surface, where the temperature is imposed.
- Thermocouple 2: is positioned at a depth of $\frac{1}{8}\Delta x$.
- Thermocouple 3: is positioned at a depth of $\frac{1}{4}\Delta x$.
- Thermocouple 4: is positioned at a depth of $\frac{1}{2}\Delta x$.
- Thermocouple 5: is positioned at the right hand surface.

For the microscopic radiation model, the thermocouples measure the average temperature of a group of elements (fibers). We use this approach because at a given position, there might not be any fiber present.

2. Microscopic radiation model

For the transient radiation model, the time-dependent evolution of the enthalpy of the fibers is accounted for and the energy equation is solved for each fiber. The results shown in Fig. 4 are the averaged (five random geometries) results for calculation 2. It is interesting to notice that the thermocouple curves 2,3 and 4 show a distinctive *bend* in the high temperature range (at $t \approx 120$ seconds). The reason for this bend is not directly obvious from looking at the full radiation equations, but the effective conductivity Eq. 14 is more explicit. As we can see from this equation, the heat flux q_r depends on both ΔT and T^3 . As a consequence at the beginning of the analysis ΔT is high and the structure heats up quickly. This effect will eventually level off, but is taken over in the high temperature range by the T^3 term.

3. Equivalent conductivity model

In the equivalent model we use the apparent density of 175.7 kg/m^3 . The model consists of a uniform mesh with a total length of Δx . We use the equivalent conductivities reported in Table 2. The results of the equivalent calculation and the radiation calculation are shown in Fig. 5. The equivalent calculation represents accurately the radiation model, even during a high heating rate transient phase.

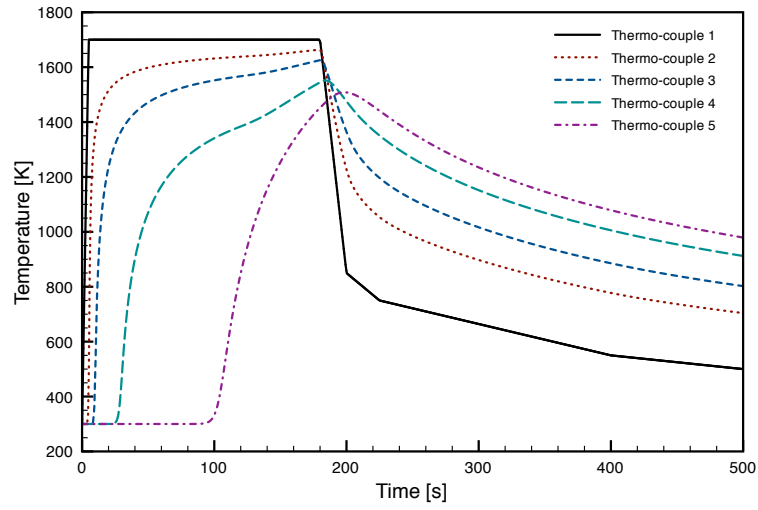


Figure 4. Average Temperature as a function of time for the radiation model ($\Delta x = 8.10^{-3}$ m).

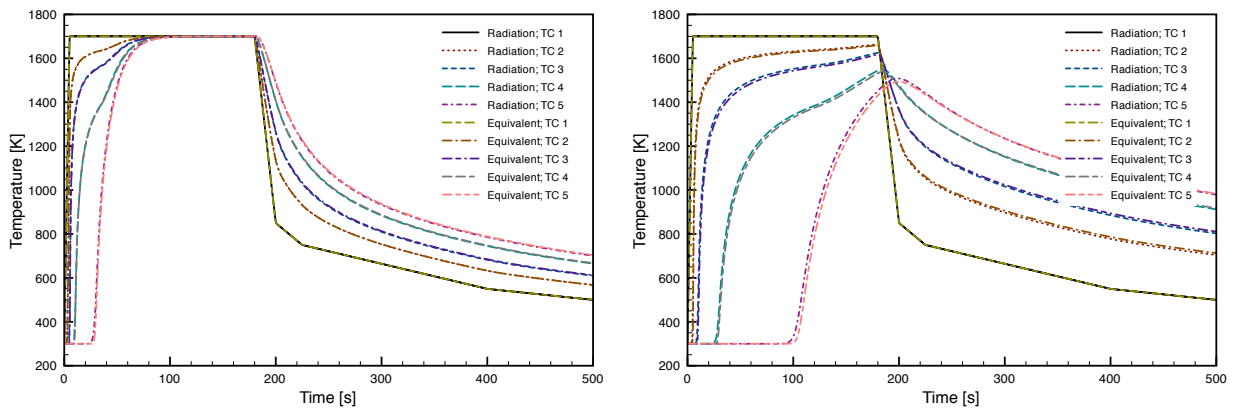


Figure 5. Comparison of the Temperature evolution for the equivalent and the radiation model, [a] Calculation 1, [b] Calculation 2.

IV. Application to ablation

INTEGRATING the proposed phenomenological model in state-of-the-art material response models is straightforward since the formulation of the heat transfer term is unchanged in the energy equation. The only difference is that the effective conductivity is now a function of the ablation zone thickness. We present in Fig. 6 three cases to illustrate the effect of the ablation zone on heat transfer. To avoid possible misinterpretations due to complex couplings, we simplify the problem to heat transfer in charred PICA:

- The material properties are extracted from a study on PICA by Covington *et al.*¹⁵ A third-order polynomial approximation of the effective conductivity of the char shows that the pre-factor of the radiative term (in T^3) is $0.97 \cdot 10^{-11} \text{ W}/(\text{m}\cdot\text{K}^4)$; that is, around twice as small as the pre-factor computed in this study for fiber preform (see Table 2). This is not surprising since the extinction coefficient is expected to be larger in the char, which is less porous.
- Neumann boundary conditions are chosen on both sides of the 1D test case represented in Fig. 6: at the surface, a heat flux of $1 \text{ MW}/\text{m}^2$ is imposed for 3 minutes; then, the cool-down is observed for 3 minutes; at the bottom, an adiabatic condition has been chosen.
- We compare three configurations:
 - A Reference case with no ablation zone.
 - B Case with an ablation zone of 0.5 mm. The pre-factor of the radiative term (in T^3), computed from Eq. 12 with $\sigma_{ext} = 63.11 \text{ m}^2/\text{kg}$, is found to lie around $1.63 \cdot 10^{-11} \text{ W}/(\text{m}\cdot\text{K}^4)$.
 - C Case with an ablation zone of 2 mm. The pre-factor of the radiative term (in T^3) is found to lie around $1.91 \cdot 10^{-11} \text{ W}/(\text{m}\cdot\text{K}^4)$. It is larger than in case B because the ablation layer (Δx) is larger.

The comparison of cases A, B, and C reveals two interesting features:

1. In the presence of the ablation zone (cases B and C), the temperature gradient in the sub-surface layer is smaller. This is very likely to enhance ablation since the heat penetrates more deeply in the material.
2. Even if the depth of the ablation zone is only of the order of 1 mm, compared to a sample of an inch (25.4 mm), the temperature profile of the thermocouple located deep in the material is affected. This should increase the pyrolysis rate, whose endothermic effect should, in turn, partially limit the observed increase of temperature at the bondline.

V. Conclusion

DIRECT numerical simulations (DNS) of the radiation heat-transfer in fibrous media have enabled us to validate a semi-analytical (phenomenological) model for the effective radiative conductivity. The effective conductivity is shown to be a function of three parameters: the local temperature (T^3), the extinction coefficient, and the sample thickness. The extinction coefficient of a 2D fiber preform made of randomly positioned but parallel fibers has been determined by inverse analysis in steady state. Transient regime simulations have been carried out using both DNS and a linear macroscopic model for heat transfer (Fourier's law). When the effective radiation conductivity computed in steady state (using DNS) is used as an input to the macroscopic model, the macroscopic model reproduces the transient DNS simulations with an appropriate level of uncertainty. Hence, the results from our study indicate that the proposed correlation can be used for both steady state and transient analysis. The results show that Rosseland hypothesis used to linearize the radiative heat transfer is correct and even very conservative in the 2D case studied.

Furthermore, the results of the fundamental study have been used to analyze the behavior of a low-density carbon/phenolic composite partially ablated. In the ablation zone, located under the surface of a thermal protection system in low-density carbon/phenolic composites, the matrix is removed and the carbon fibers lie unprotected. The effective radiative conductivity is found to be about twice as large in the ablation zone. The integration of the proposed model in state-of-the-art ablation tools is very easy since only the effective conductivity needs to be modified (the formulation of the energy equation is not modified). The effect of the ablation zone on the temperature profile in the material is found to be very slight but noticeable.

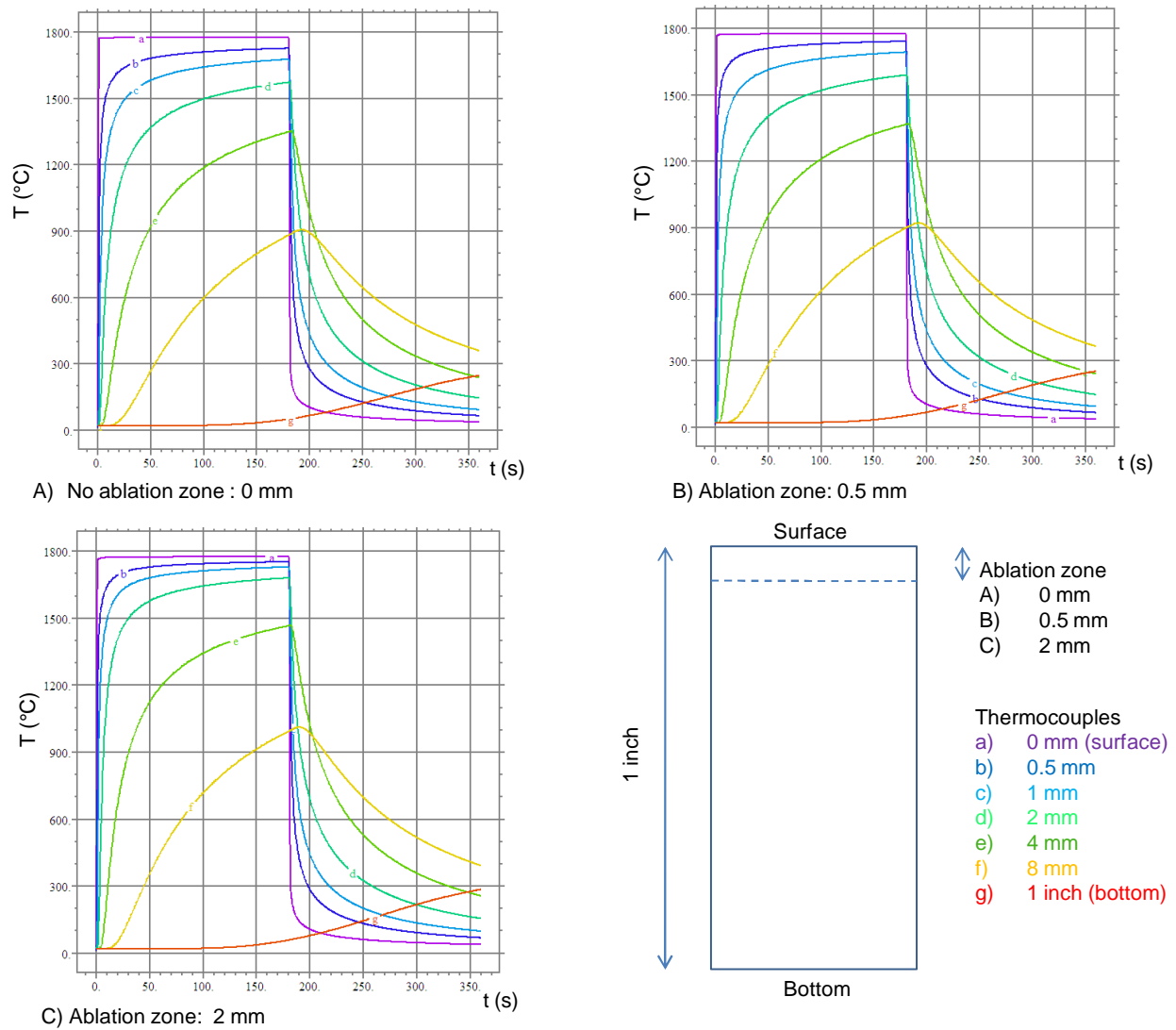


Figure 6. Effect of the thickness of the ablation zone on the temperature profile (Heat flux: 1 MW/m^2).

Current material response models are not yet ready to compute the ablation zone thickness; however, they compute the char layer thickness. The approach of this paper may also be used in the prediction of the effective radiative conductivity of the char layer. The only difference is that the extinction coefficient is larger by at least a factor of two compared to raw fiber preforms. Therefore, the effective conductivity can be considered constant for char layers thicker than 1 mm (against 2 mm for the optically thinner fiber preform in the ablation zone). Assuming a constant effective conductivity of the char layer (experimentally measured on thick samples), is a conservative hypothesis, which leads to a slight overestimation of the bondline temperature. On the other hand, ignoring the presence of the ablation zone (if any) would lead to a slight underestimation of the bondline temperature.

As a perspective to this work, we would like to:

1. extend the study to 3D fibrous architecture;
2. carry out DNS simulations on real architectures extracted from computed micro-tomographies;
3. implement the results in a pyrolysis-ablation material-response code.

References

- ¹Stackpoole, M., Sepka, S., Cozmuta, I., and Kontinos, D., "Post-Flight Evaluation of Stardust Sample Return Capsule Forebody Heatshield Material," AIAA paper 2008-1202, Jan. 2008.
- ²Ritter, H., Portela, P., Keller, K., Bouilly, J. M., and Burnage, S., "Development of a European ablative material for heatshields of sample return missions," 6th European Workshop on TPS and Hot structures, Stuttgart, Germany, 1-3 April 2009.
- ³Lachaud, J., Cozmuta, I., and Mansour, N. N., "Multiscale Approach to Ablation Modeling of Phenolic Impregnated Carbon Ablators," *Journal of Spacecraft and Rockets*, under press.
- ⁴Lachaud, J. and Mansour, N. N., "Microscopic scale simulation of the ablation of fibrous materials," *Proc. 48th AIAA Aerospace Sciences Meeting*, AIAA, Jan. 2010, to appear.
- ⁵Lee, S. C., "Radiation heat-transfer model for fibers oriented parallel to diffuse boundaries," *Journal of Thermophysics*, Vol. 2, 1988, pp. 303-308.
- ⁶Petrov, V. A., "Combined radiation and conduction heat transfer in high temperature fiber thermal insulation," *International journal of heat and mass transfer*, Vol. 40, 1994, pp. 2241-2247.
- ⁷Lee, S. C. and Cunningham, G. R., "Conduction and radiation heat transfer in high-porosity fiber thermal insulation," *Journal of thermophysics and heat transfer*, Vol. 14, 2000, pp. 121-136.
- ⁸Bankvall, C., "Heat transfer in fibrous materials," *Journal of testing and evaluation*, Vol. 1, 1973, pp. 235-243.
- ⁹Banas, R. P. and Cunningham, G. R., "Determination of the effective thermal conductivity for the space shuttle orbiter's reusable surface insulation," AIAA paper 1974-730, Jul. 1974.
- ¹⁰Marschall, J., Maddren, J., and Parks, J., "Internal radiation transport and effective thermal conductivity of fibrous ceramic insulation," AIAA paper 2001-2822, Jun. 2001.
- ¹¹Zeeb, C., *Performance and accuracy enhancements of radiative heat transfer modeling via Monte Carlo*, PhD thesis, Colorado State University, 2002.
- ¹²Modest, M. F., *Radiative Heat Transfer*, McGraw-Hill, New York, 1993, 2nd edition.
- ¹³Plotard, P. and Labaste, V., "Entry system development for Mars Netlander mission," *Acta Astronautica*, Vol. 55, 2004, pp. 677-686.
- ¹⁴Deissler, R. G., "Diffusion approximation for thermal radiation in gases with jump boundary condition," *Proc. ASME-AIChE Heat transfer conference*, No. 63-HT-13, 1963.
- ¹⁵Covington, M. A., Heinemann, J. M., Chen, Y.-K., Terrazas-Salinas, I., Balboni, J. A., Olejniczak, J., and Martinez, E. R., "Performance of a Low Density Ablative Heat Shield Material," *Journal of Spacecrafts and Rockets*, Vol. 45, No. 4, 2008, pp. 856-864.